Energy-efficient Rate Splitting for MIMO STAR-RIS-assisted Broadcast Channels with I/Q Imbalance

Mohammad Soleymani*, Ignacio Santamaria†, and Eduard Jorswieck‡

*Signal & System Theory Group, Universität Paderborn, Germany
†Dept. Communications Engineering, Universidad de Cantabria, Spain
‡ Institute for Communications Technology, Technische Universität Braunschweig, Germany
Email: mohammad.soleymani@sst.upb.de, i.santamaria@unican.es, jorswieck@ifn.ing.tu-bs.de

Abstract—**This paper proposes an energy-efficient scheme for multicell multiple-input, multiple-output (MIMO) simultaneous transmit and reflect (STAR) reconfigurable intelligent surfaces (RIS)-assisted broadcast channels by employing rate splitting (RS) and improper Gaussian signaling (IGS). Regular RISs can only reflect signals. Thus, a regular RIS can assist only when the transmitter and receiver are in the reflection space of the RIS. However, a STAR-RIS can simultaneously transmit and reflect, thus providing a $360°$ coverage. In this paper, we assume that transceivers may suffer from I/Q imbalance (IQI). To compensate for IQI, we employ IGS. Moreover, we employ RS to manage intracell interference. We show that RIS can significantly improve the energy efficiency (EE) of the system when RIS components are carefully optimized. Additionally, we show that STAR-RIS can significantly outperform a regular RIS when the regular RIS cannot cover all the users. We also show that RS can highly increase the EE comparing to treating interference as noise.**

Index Terms—**Energy efficiency, improper Gaussian signaling, majorization minimization, MIMO broadcast channels, rate splitting, reflecting intelligent surface.**

I. INTRODUCTION

Among the main targets of 6G is to improve the energy efficiency (EE) by a factor of $10 \sim 100$ times higher than the EE of 5G networks [1]. A promising technology to improve EE is reconfigurable intelligent surface (RIS), which can provide extra degrees of freedom by optimizing the propagation channels or generally the environment [2], [3]. Another promising technology to improve EE and/or spectral efficiency (SE) is rate splitting (RS), which is a powerful interference-management technique that includes many other techniques such as treating interference as noise (TIN), spatial division multiple access (SDMA), and non-orthogonal multiple access (NOMA) [4]. This paper employs RS and RIS to enhance the EE of a multi-cell broadcast channel (BC).

RIS has been shown to improve EE and SE of various networks [5]–[11]. RIS can modulate channels, thus improving the coverage or reducing/neutralizing the interference. Hence, there can be different applications for RIS in a network. For instance, RIS can manage interference in some specific scenarios such as K-user interference channels [10], [11]. Moreover, RIS can strengthen the cell-edge links (either in interference-free or interference-limited systems), which can highly improve the minimum rate and or EE of the network.

A regular passive RIS can only reflect signals, which may restrict its coverage range. Indeed, both transceivers should be in the reflection space of a regular RIS so that it can modulate the channel. To address this issue, simultaneously reflect and transmit RIS (STAR-RIS) is proposed that can reflect and transmit simultaneously, which provides a full $360°$ coverage [12]–[16]. Thus, STAR-RIS may be able to support a wider range of applications compared to a regular RIS.

RIS can manage intercell interference in a multi-cell BC. However, RIS cannot fully mitigate intracell interference especially when a network is over loaded, i.e., when the number of users per cell is higher than the number of base station (BS) antennas [8], [17], [18]. Thus, the system performance can be improved if other interference management techniques such as RS are employed in RIS-assisted systems. We refer the reader to [4] for a more detailed overview on RS.

Another main obstacle to improve EE and/or SE is hardware impairment (HWI). In practice, devices are never completely ideal, which can significantly degrade the system performance especially when such impairments are not compensated [19]–[21]. A source of HWI is an imbalance in in-phase and quadrature branches, which is known as I/Q imbalance (IQI) [20], [21]. When IQI occurs, the output signal can be modeled as a widely linear transformation of the input signals, which may make the signals and noise improper. To compensate for IQI, we can employ improper Gaussian signaling (IGS), which is also an interference-management technique [20], [22]–[26].

In this paper, we employ the 1-layer RS alongside with IGS to improve EE of a multicell STAR-RIS-assisted BC with IQI. In [17], we proposed a framework for RS in RIS-assisted systems by mainly studying a regular RIS. In this work, we focus on STAR-RIS and propose energy-efficient RS schemes for different operational modes of STAR-RIS by considering three different feasibility sets. We consider two schemes for STAR-RIS. First, we assume that each STAR-RIS component can simultaneously transmit and reflect, which is known as energy splitting (ES). Second, we randomly divide STAR-RIS components into two sets. In the first set, we assume that all components can only reflect, while in the second set, all components can only transmit. This scheme is known as mode switching (MS). We show that the joint RS and RIS design
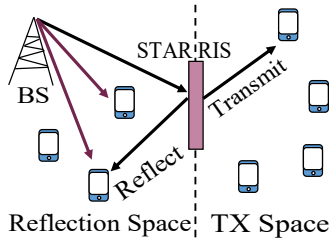
Fig. 1: A typical STAR-RIS-assisted system.

significantly increases the EE of the system. Moreover, we show that STAR-RIS can highly outperform a regular RIS with a relatively low number of RIS components when the regular RIS cannot cover all the users. The MS scheme can perform very close to the ES scheme for more realistic feasibility sets for RIS components in the considered scenario.

II. SYSTEM MODEL

We consider a multi-cell MIMO STAR-RIS-assisted BC with L multiple-antenna BSs, each serving K users with N_u receive antennas. Each BS has N_{BS} transmit antennas. We assume that there are M passive STAR-RISs with N_{RIS} elements to assist the communications. We further assume that each transceiver suffers from IQI based on the model in [21]. For notational simplicity, we consider a symmetric scenario without a loss of generality. However, the proposed scheme can be easily extended to asymmetric systems.

A. STAR-RIS model

In a STAR-RIS-assisted system, each user belongs to either reflection space or transmission space (see Fig. 1). Hence, the channel between BS i and the k-th user associated to BS l (denoted by u_{lk}) is [14, Eq. (2)]

$$\mathbf{H}_{lk,i} = \underbrace{\sum_{m=1}^{M} \mathbf{G}_{lk,m} \boldsymbol{\Theta}_m^{r/t} \mathbf{G}_{mi}}_{\text{links through STAR-RIS}} + \underbrace{\mathbf{F}_{lk,i}}_{\text{direct link}}, \quad (1)$$

where $\mathbf{G}_{lk,m}$ is the channel matrix between the m-th RIS and u_{lk}, $\mathbf{F}_{lk,i}$ is the direct channel between BS i and u_{lk}, and $\mathbf{G}_{mi}$ is the channel matrix between RIS m and BS i. The matrix $\boldsymbol{\Theta}_m^r$ (or $\boldsymbol{\Theta}_m^t$) is a diagonal matrix containing the reflection (or transmission) coefficient of each RIS component. In other words, $\boldsymbol{\Theta}_m^r = \mathrm{diag}\left(\theta_{m_1}^r, \theta_{m_2}^r, \cdots, \theta_{m_{N_{RIS}}}^r\right)$, and $\boldsymbol{\Theta}_m^t = \mathrm{diag}\left(\theta_{m_1}^t, \theta_{m_2}^t, \cdots, \theta_{m_{N_{RIS}}}^t\right)$, where $\theta_{m_i}^r$ (or $\theta_{m_i}^t$) is the reflection (or transmission) coefficient of the i-th STAR-RIS component. If a user is in the reflection (or transmission) space of a STAR-RIS, the channel for the user can be controlled by $\theta_{m_i}^r$ (or $\theta_{m_i}^t$). Unfortunately, the reflection and transmission coefficients of each RIS component are dependent. There are three models for the relation between $\theta_{m_i}^r$ and $\theta_{m_i}^t$. In the first model, the amplitudes of $\theta_{m_i}^r$ and $\theta_{m_i}^t$ are related to each other as in the set [15, Eq. (2)]

$$\mathcal{T}_U = \left\{ \theta_{m_i}^r, \theta_{m_i}^t : |\theta_{m_i}^r|^2 + |\theta_{m_i}^t|^2 \leq 1 \ \forall m, i \right\}. \quad (2)$$

The set $\mathcal{T}_U$ is convex. In another model, the amplitudes of $\theta_{m_i}^r$ and $\theta_{m_i}^t$ are related to each other as in the set [27, Eq. (1)]

$$\mathcal{T}_I = \left\{ \theta_{m_i}^r, \theta_{m_i}^t : |\theta_{m_i}^r|^2 + |\theta_{m_i}^t|^2 = 1 \ \forall m, i \right\}. \quad (3)$$

In the sets $\mathcal{T}_U$ and $\mathcal{T}_I$, the phases of $\theta_{m_i}^r$ and $\theta_{m_i}^t$ can be independently optimized. In another model, not only the amplitudes of $\theta_{m_i}^r$ and $\theta_{m_i}^t$ are dependent, but also their phases are related as in the following set [12], [16, Lemma 1]

$$\mathcal{T}_N = \left\{ \theta_{m_i}^r, \theta_{m_i}^t : |\theta_{m_i}^r|^2 + |\theta_{m_i}^t|^2 = 1, |\theta_{m_i}^r \pm \theta_{m_i}^t|^2 \leq 1, \forall m, i \right\}.$$

There are three different modes for operating a STAR-RIS. First, each STAR-RIS component can simultaneously reflect and transmit, which is known as the ES scheme. Second, a set of STAR-RIS components operate only in the transmission mode and the other components operate only the reflection mode, which is known as the MS scheme. Third, all STAR-RIS components operate in the transmission mode in a time slot, and then they operate in the reflection mode in the next time slot, which is known as the time switching (TS) scheme. In this paper, we do not consider the TS scheme since it operates similar to a regular RIS in each time slot, and may not provide a considerable gain over a regular RIS when time sharing among users is not allowed [16].

B. Signal model

In this paper, we consider the 1-layer RS in which each BS transmits two types of messages, i.e., common and private. Thus, the BS intends to transmit $\mathbf{x}_l = \mathbf{x}_{c,l} + \sum_k \mathbf{x}_{lk}$, where $\mathbf{x}_{c,l}$ is the common message, which is decoded by all the users associated to the l-th BS. Moreover, $\mathbf{x}_{lk}$ is the private message for u_{lk}. The signals $\mathbf{x}_{c,l}$ and $\mathbf{x}_{lk}$ for all l, k are zero-mean independent improper Gaussian signals. As BS l suffers from IQI, the actual transmitted signal of BS l is a widely linear transformation of $\mathbf{x}_l$, i.e., $\mathbf{x}_{tl} = \boldsymbol{\Gamma}_{1t}\mathbf{x}_l + \boldsymbol{\Gamma}_{2t}\mathbf{x}_l^*$, where $\boldsymbol{\Gamma}_{1t}$ and $\boldsymbol{\Gamma}_{2t}$ are given by [20, Eq. (7)] and [20, Eq. (8)], respectively. The received signal at u_{lk} is $\mathbf{y}_{rlk} = \sum_{i=1}^{L} \mathbf{H}_{lk,i} \left(\boldsymbol{\Gamma}_{1t}\mathbf{x}_l + \boldsymbol{\Gamma}_{2t}\mathbf{x}_l^* \right) + \mathbf{n}_{lk}$, where $\mathbf{n}_{lk}$ is zero-mean white additive proper Gaussian noise. Due to IQI at the receiver of u_{lk}, the actual received signal at u_{lk} is a widely linear transform of $\mathbf{y}_{rlk}$ as $\mathbf{y}_{lk} = \boldsymbol{\Gamma}_{1r}\mathbf{y}_{rlk} + \boldsymbol{\Gamma}_{2r}\mathbf{y}_{rlk}^*$, where $\boldsymbol{\Gamma}_{1r}$ and $\boldsymbol{\Gamma}_{2r}$ are given by [20, Eq. (12)] and [20, Eq. (13)], respectively. To deal with impropriety, we employ the real-decomposition method in which every signal/parameter is written in a real domain. Employing [20, Lemma 1], the received signal at u_{lk} can be written as $\underline{\mathbf{y}}_{lk} = \sum_{i=1}^{L} \underline{\mathbf{H}}_{lk,i}\underline{\mathbf{x}}_i + \underline{\mathbf{n}}_{lk}$, where the parameters are defined as in [17, Eq. (2)].

C. Rate and energy efficiency expressions

The rate of u_{lk} is the summation of the achievable rate of its private message, $\mathbf{x}_{lk}$, and its dedicated rate from the common message, $\mathbf{x}_{c,l}$, as $r_{lk} = r_{p,lk} + r_{c,lk}$, where $r_{p,lk}$ is the rate of the private message $\mathbf{x}_{lk}$ after decoding and canceling the common message $\mathbf{x}_{c,l}$ while treating the other interfering signals as noise, i.e.,

$$r_{p,lk} = \frac{1}{2}\log_2\left|\mathbf{I} + \mathbf{D}_{lk}^{-1}\mathbf{S}_{lk}\right| = \underbrace{\frac{1}{2}\log_2|\mathbf{D}_{lk} + \mathbf{S}_{lk}|}_{r_{p,lk_1}} - \underbrace{\frac{1}{2}\log_2|\mathbf{D}_{lk}|}_{r_{p,lk_2}},$$

1505

where $\mathbf{S}_{lk} = \underline{\mathbf{H}}_{lk,l}\mathbf{P}_{lk}\underline{\mathbf{H}}_{lk,l}^T$, and

$$\mathbf{D}_{lk} = \underbrace{\sum_{i=1,i\neq l}^{L} \underline{\mathbf{H}}_{lk,i}\mathbf{P}_i\underline{\mathbf{H}}_{lk,i}^T}_{\text{Intercell interference}} + \underbrace{\sum_{j=1,j\neq k}^{K} \underline{\mathbf{H}}_{lk,l}\mathbf{P}_{lj}\underline{\mathbf{H}}_{lk,l}^T}_{\text{Intracell interference}} + \underbrace{\underline{\mathbf{C}}_n}_{\text{Noise}},$$

where $\underline{\mathbf{C}}_n$ is the covariance matrix of the noise $\underline{\mathbf{n}}_{lk}$, i.e., $\underline{\mathbf{C}}_n = \mathbb{E}\{\underline{\mathbf{n}}_{lk}\underline{\mathbf{n}}_{lk}^T\}$, and $\mathbf{P}_i = \mathbf{P}_{c,i} + \sum_k \mathbf{P}_{ik}$ for all i, where $\mathbf{P}_{c,i}$, and $\mathbf{P}_{ik}$ are, respectively, the transmit covariance matrix of $\underline{\mathbf{x}}_{c,i}$ and $\underline{\mathbf{x}}_{ik}$. The term $r_{c,lk} \geq 0$ in r_{lk} refers to the portion of the common rate allocated to u_{lk}. The common message $\underline{\mathbf{x}}_{c,l}$ should be decodable by all users associated to BS l. Thus, the transmission rate of the common message at BS l should be chosen according to

$$r_l = \sum_{k=1}^{K} r_{c,lk} \leq \min_k \{\bar{r}_{c,lk}\} \triangleq r_{c,l}, \tag{4}$$

where $\bar{r}_{c,lk}$ is the maximum decodable rate of $\underline{\mathbf{x}}_{c,l}$ at u_{lk} treating the other signals as noise

$$\bar{r}_{c,lk} = \underbrace{\frac{1}{2}\log_2|\mathbf{D}_{c,lk} + \mathbf{S}_{c,lk}|}_{\bar{r}_{c,lk_1}} - \underbrace{\frac{1}{2}\log_2|\mathbf{D}_{c,lk}|}_{\bar{r}_{c,lk_2}},$$

where $\mathbf{S}_{c,lk} = \underline{\mathbf{H}}_{lk,l}\mathbf{P}_{l,c}\underline{\mathbf{H}}_{lk,l}^T$ and $\mathbf{D}_{c,lk} = \mathbf{S}_{lk} + \mathbf{D}_{lk}$.

The EE of a user is defined as the ratio between its rate and total consumed energy to transmit its data as [28]

$$e_{lk} = \frac{r_{lk}}{P_c + \eta\text{Tr}(\mathbf{P}_{lk} + \mathbf{P}_{c,l}/K)}, \tag{5}$$

where $1/\eta$ is the power efficiency of the BSs and P_c is the constant power consumption for transmitting data to a user, given by [8, Eq. (27)].

D. Problem statement

In this paper, we maximize the minimum-weighted EE (MWEE) of users:

$$\max_{\{\mathbf{P}\}\in\mathcal{P},\{\boldsymbol{\Theta}\}\in\mathcal{T},\mathbf{r}_c,e} e \text{ s.t. } e_{lk} \geq \alpha_{lk}e, \; \forall lk, \tag{6a}$$

$$\sum_k r_{c,lk} \leq \min_k\{\bar{r}_{c,lk}\} = r_{c,l}, \forall l, \tag{6b}$$

$$r_{c,lk} \geq 0, \; r_{lk} \geq r_{lk}^{th}, \; \forall lk, \tag{6c}$$

where $\mathbf{r}_c = \{r_{c,lk}\}_{\forall lk}$, $\{\mathbf{P}\} = \{\mathbf{P}_{lk}, \mathbf{P}_{c,l}\}_{\forall lk}$, and $\{\boldsymbol{\Theta}\} = \{\boldsymbol{\Theta}_m^r, \boldsymbol{\Theta}_m^t\}_{\forall m}$ are the optimization variables. Moreover, α_{lk} is the weight for u_{lk}, which corresponds to the priority of the user. The set $\mathcal{P}$ includes all the feasible transmit covariance matrices and is given by [17, Eq. (3)]. Moreover, $\mathcal{T}$ is the feasibility set for RIS components, which can be $\mathcal{T}_U$, $\mathcal{T}_I$, or $\mathcal{T}_N$.

III. PROPOSED RATE SPLITTING SCHEME

The optimization problem (6) is non-convex and difficult. In this section, we find a suboptimal solution for (6) by employing an iterative approach based on majorization minimization (MM) and alternating optimization (AO) to approximate (6). That is, we first fix the RIS components, $\{\boldsymbol{\Theta}^{(t-1)}\} = \{\boldsymbol{\Theta}^{r^{(t-1)}}, \boldsymbol{\Theta}^{t^{(t-1)}}\}$, and solve (6) over transmit

covariance matrices to obtain $\{\mathbf{P}^{(t)}\}$. We then solve (6) over RIS components for given transmit covariance matrices, $\{\mathbf{P}^{(t)}\}$, to find $\{\boldsymbol{\Theta}^{(t)}\}$. We iterate this procedure until a convergence condition is met.

A. Optimizing transmit covariance matrices

The optimization problem (6) is non-convex even for fixed $\{\boldsymbol{\Theta}^{(t-1)}\}$ since the rates are not concave in $\{\mathbf{P}\}$. To solve (6) for fixed $\{\boldsymbol{\Theta}^{(t-1)}\}$, we first find suitable surrogate functions for the rates by employing convex-concave procedure (CCP) since the rates can be written as a difference two concave functions in $\{\mathbf{P}\}$. To this end, we employ [17, Lemma 3], which results in

$$r_{p,lk} \geq \tilde{r}_{p,lk} = r_{p,lk_1}(\{\mathbf{P}\}) - r_{p,lk_2}^{(t-1)}$$
$$- \sum_{j=1,\neq k}^{K}\text{Tr}\left(\frac{\mathbf{H}_{lk,l}^T(\mathbf{D}_{lk}^{(t-1)})^{-1}\mathbf{H}_{lk,l}}{2\ln 2}\left(\mathbf{P}_{lj} - \mathbf{P}_{lj}^{(t-1)}\right)\right)$$
$$- \sum_{i=1,\neq l}^{L}\text{Tr}\left(\frac{\mathbf{H}_{lk,i}^T(\mathbf{D}_{lk}^{(t-1)})^{-1}\mathbf{H}_{lk,i}}{2\ln 2}\left(\mathbf{P}_i - \mathbf{P}_i^{(t-1)}\right)\right),$$

$$\bar{r}_{c,lk} \geq \tilde{r}_{c,lk} = r_{c,lk_1}(\{\mathbf{P}\}) - r_{c,lk_2}^{(t-1)}$$
$$- \sum_{j=1}^{K}\text{Tr}\left(\frac{\mathbf{H}_{lk,l}^T(\mathbf{D}_{c,lk}^{(t-1)})^{-1}\mathbf{H}_{lk,l}}{2\ln 2}\left(\mathbf{P}_{lj} - \mathbf{P}_{lj}^{(t-1)}\right)\right)$$
$$- \sum_{i=1,\neq l}^{L}\text{Tr}\left(\frac{\mathbf{H}_{lk,i}^T(\mathbf{D}_{c,lk}^{(t-1)})^{-1}\mathbf{H}_{lk,i}}{2\ln 2}\left(\mathbf{P}_i - \mathbf{P}_i^{(t-1)}\right)\right),$$

where $r_{p,lk_2}^{(t-1)} = r_{p,lk_2}(\{\mathbf{P}^{(t-1)}\})$, $\mathbf{D}_{lk}^{(t-1)} = \mathbf{D}_{lk}(\{\mathbf{P}^{(t-1)}\})$, $r_{c,lk_2}^{(t-1)} = r_{c,lk_2}(\{\mathbf{P}^{(t-1)}\})$, and $\mathbf{D}_{c,lk}^{(t-1)} = \mathbf{D}_{c,lk}(\{\mathbf{P}^{(t-1)}\})$. Substituting the rates with the concave lower bounds in (6) for fixed $\{\boldsymbol{\Theta}^{(t-1)}\}$ yields

$$\max_{\{\mathbf{P}\}\in\mathcal{P},\mathbf{r}_c,e} e \text{ s.t. } \frac{\tilde{r}_{lk}}{P_c + \eta\text{Tr}(\mathbf{P}_{lk} + \mathbf{P}_{c,l}/K)} \geq \alpha_{lk}e, \; \forall lk, \tag{7a}$$

$$\sum_k r_{c,lk} \leq \min_k\{\tilde{r}_{c,lk}\} = r_{c,l}, \forall l, \tag{7b}$$

$$r_{c,lk} \geq 0, \; \tilde{r}_{lk} \geq r_{lk}^{th}, \; \forall lk, \tag{7c}$$

which is non-convex, but its global optimal solution can be obtained by the generalized Dinkelbach algorithm [28]. Due to a space restriction, we do not provide details and refer the reader to, e.g., [28].

B. Optimizing RIS components

In the following, we first consider the ES scheme. Then, we mention how the scheme can be adapted to the MS scheme, which is a special case of the ES scheme. For fixed $\{\mathbf{P}^{(t)}\}$, (6) is non-convex since the rates are not concave in $\{\boldsymbol{\Theta}\}$, and the set $\mathcal{T}$ is non-convex for $\mathcal{T}_I$ and $\mathcal{T}_N$. To solve (6) for fixed $\{\mathbf{P}^{(t)}\}$, we first obtain a concave lower bound for the rates by applying [8, Lemma 2] as

$$r_{p,lk} \geq \hat{r}_{p,lk} = r_{p,lk}^{(t-1)} - \frac{1}{2\ln 2}\left(\text{Tr}(\bar{\mathbf{S}}_{lk}\bar{\mathbf{D}}_{lk}^{-1}) + 2\text{Tr}(\bar{\mathbf{V}}_{lk}^T\bar{\mathbf{D}}_{lk}^{-1}\mathbf{V}_{lk})\right.$$
$$\left. - \text{Tr}((\bar{\mathbf{D}}_{lk}^{-1} - (\bar{\mathbf{S}}_{lk} + \bar{\mathbf{D}}_{lk})^{-1})^T(\mathbf{S}_{lk} + \mathbf{D}_{lk}))\right),$$

$$\bar{r}_{c,lk} \geq \hat{r}_{c,lk} = r_{c,lk}^{(t-1)} - \frac{1}{2\ln 2}\Big(\text{Tr}\Big(\bar{\mathbf{S}}_{c,lk}\bar{\mathbf{D}}_{c,lk}^{-1}\Big) + 2\text{Tr}\Big(\bar{\mathbf{V}}_{c,lk}^T\bar{\mathbf{D}}_{c,lk}^{-1}$$

$$\times \mathbf{V}_{c,lk}\Big) - \text{Tr}\Big((\bar{\mathbf{D}}_{c,lk}^{-1} - (\bar{\mathbf{S}}_{c,lk}+\bar{\mathbf{D}}_{c,lk})^{-1})^T(\mathbf{S}_{c,lk}+\mathbf{D}_{c,lk})\Big)\Big),$$

where $\mathbf{V}_{lk} = \underline{\mathbf{H}}_{lk,l}\mathbf{P}_{lk}^{(t)1/2}$, $\bar{\mathbf{V}}_{lk} = \underline{\mathbf{H}}_{lk,l}\left(\{\boldsymbol{\Theta}\}^{(t-1)}\right)\mathbf{P}_{lk}^{(t)1/2}$, $\bar{\mathbf{D}}_{lk} = \mathbf{D}_{lk}\left(\{\boldsymbol{\Theta}\}^{(t-1)}\right)$, $\mathbf{V}_{c,lk} = \underline{\mathbf{H}}_{lk,l}\mathbf{P}_{c,l}^{(t)1/2}$, $\bar{\mathbf{V}}_{c,lk} = \mathbf{S}_{c,lk}^{1/2}\left(\{\boldsymbol{\Theta}\}^{(t-1)}\right)$, and $\bar{\mathbf{D}}_{c,lk} = \mathbf{D}_{c,lk}\left(\{\boldsymbol{\Theta}\}^{(t-1)}\right)$. Inserting the concave lower bounds for the rates into (6) for fixed $\{\mathbf{P}^{(t)}\}$ results in

$$\max_{\{\boldsymbol{\Theta}\}\in\mathcal{T},\mathbf{r}_c,e} e \quad \text{s.t.} \quad \frac{\hat{r}_{lk}}{P_c + \eta\text{Tr}(\mathbf{P}_{lk}+\mathbf{P}_{c,l}/K)} \geq \alpha_{lk}e, \ \forall lk, \quad (8a)$$

$$\sum_k r_{c,lk} \leq \min_k\{\hat{r}_{c,lk}\} = r_{c,l}, \forall l, \quad (8b)$$

$$r_{c,lk} \geq 0, \ \hat{r}_{lk} \geq r_{lk}^{th}, \ \forall lk, \quad (8c)$$

which is convex only when $\mathcal{T}$ is a convex set, i.e., when $\mathcal{T} = \mathcal{T}_U$. In this case, the proposed algorithm converges to a stationary point of (6) for both ES and MS schemes since the surrogate functions for the rates fulfill the three conditions in [20, Sec. III]. We propose a suboptimal approach to convexify $\mathcal{T}_I$ and $\mathcal{T}_N$ below.

The sets $\mathcal{T}_I$ and $\mathcal{T}_N$ are not convex due to the constraint $|\theta_{m_i}^r|^2 + |\theta_{m_i}^t|^2 = 1$, which can be written as the two constraints: $|\theta_{m_i}^r|^2 + |\theta_{m_i}^t|^2 \leq 1$ and $|\theta_{m_i}^r|^2 + |\theta_{m_i}^t|^2 \geq 1$. The former is a convex constraint, but the latter is not since $|\theta_{m_i}^r|^2 + |\theta_{m_i}^t|^2$ is a convex function, instead of being concave. Thus, we can apply CCP to convexify this constraint as

$$\zeta(\theta_{m_i}^r, \theta_{m_i}^t) \triangleq |\theta_{m_i}^{r(t-1)}|^2 + 2\Re\left(\theta_{m_i}^{r(t-1)}(\theta_{m_i}^r - \theta_{m_i}^{r(t-1)})^*\right) +$$

$$|\theta_{m_i}^{t(t-1)}|^2 + 2\Re\left(\theta_{m_i}^{t(t-1)}(\theta_{m_i}^t - \theta_{m_i}^{t(t-1)})^*\right) \geq 1. \quad (9)$$

To make the convergence faster, we can relax (9) by introducing $\epsilon > 0$ as $\zeta(\theta_{m_i}^r, \theta_{m_i}^t) \geq 1 - \epsilon$. Thus, we can approximate (8) for $\mathcal{T}_I$ as

$$\max_{\{\boldsymbol{\Theta}\}\in\mathcal{T},\mathbf{r}_c,e} e \quad \text{s.t.} \quad (8a) - (8c), \ \zeta(\theta_{m_i}^r, \theta_{m_i}^t) \geq 1 - \epsilon, \forall m_i, \quad (10a)$$

$$|\theta_{m_i}^r|^2 + |\theta_{m_i}^t|^2 \leq 1, \ \forall m_i, \quad (10b)$$

which is convex and can be efficiently solved. Note that for the feasibility set $\mathcal{T}_N$, we should add the convex constraints $|\theta_{m_i}^r \pm \theta_{m_i}^t|^2 \leq 1$ for all m_i, to (10) to ensure that $\angle\theta_{m_i}^r = \angle\theta_{m_i}^r \pm \pi/2$. Since these constraints are convex, the resulting problem is convex for $\mathcal{T}_N$. We call the solution of (10) for $\mathcal{T}_I$ (or $\mathcal{T}_N$) as $\boldsymbol{\Theta}_m^{r(\star)}$ and $\boldsymbol{\Theta}_m^{t(\star)}$, which may not be feasible due to the relaxation. To obtain a feasible point, we project $\boldsymbol{\Theta}_m^{r(\star)}$ and $\boldsymbol{\Theta}_m^{t(\star)}$ onto $\mathcal{T}_I$ (or $\mathcal{T}_N$) as

$$\hat{\theta}_{m_i}^t = \frac{\theta_{m_i}^{t(\star)}}{\sqrt{|\theta_{m_i}^{t(\star)}|^2 + |\theta_{m_i}^{r(\star)}|^2}}, \quad \hat{\theta}_{m_i}^r = \frac{\theta_{m_i}^{r(\star)}}{\sqrt{|\theta_{m_i}^{t(\star)}|^2 + |\theta_{m_i}^{r(\star)}|^2}}, \quad (11)$$

for all m_i. Finally, we update $\boldsymbol{\Theta}_m^r$ and $\boldsymbol{\Theta}_m^t$ such that the solution of the scheme is non-decreasing, i.e., as

$$\{\boldsymbol{\Theta}^{(t)}\} = \begin{cases} \{\hat{\boldsymbol{\Theta}}\} & \text{if} \quad \min_{lk}\left\{e_{lk}\left(\{\hat{\boldsymbol{\Theta}}\}\right)/\alpha_{lk}\right\} \geq \\ & \quad \min_{lk}\left\{e_{lk}(\{\boldsymbol{\Theta}^{(t-1)}\})/\alpha_{lk}\right\} \\ \{\boldsymbol{\Theta}^{(t-1)}\} & \text{Otherwise}, \end{cases} \quad (12)$$
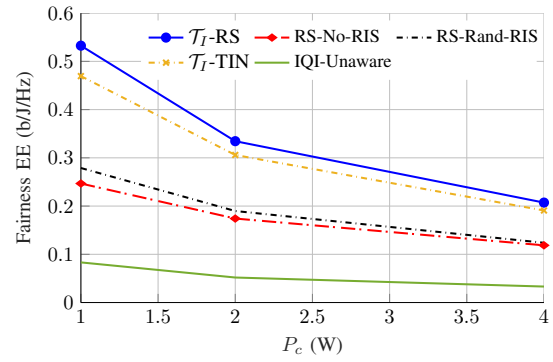

Fig. 2: The average fairness EE versus P_c for $N_{BS} = N_u = 2$, $N_{RIS} = 20$, $L = 2$, $M = 2$ and $K = 4$.

where $\{\hat{\boldsymbol{\Theta}}\} = \{\hat{\boldsymbol{\Theta}}^r, \hat{\boldsymbol{\Theta}}^t\}$ is given by (11). The convergence of the proposed scheme is ensured by (12).

In the MS scheme, we assume that a set of the RIS components operate only in the reflection mode ($\theta_{m_i}^t = 0$), while the other RIS components operate only in the transmission mode ($\theta_{m_i}^r = 0$). Hence, the proposed scheme for the ES scheme can be applied to the MS scheme by enforcing $\theta_{m_i}^t$ (or $\theta_{m_i}^r$) to zero for the set of RIS components, operating in the reflection (or transmission) mode.

Note that the number of optimization parameters decreases by half in the MS scheme, which reduces the computational complexities of the scheme. Additionally, from a practical point of view, it might be easier to operate in only transmission or reflection mode for a STAR-RIS component. However, the MS scheme can be considered as lower bound for the performance of the ES scheme since MS is a special case of ES. In other words, an optimal ES scheme never performs worse than any MS scheme since the solution of an MS scheme is a valid solution for an ES scheme.

IV. NUMERICAL RESULTS

In this section, the simulation parameters are chosen similar to [8]. In Fig. 2, we show the average fairness EE versus P_c for $N_{BS} = N_u = 2$, $N_{RIS} = 20$, $L = 2$, $M = 2$ and $K = 2$. In this figure, we consider a two-cell system with one RIS in each cell, as shown in [8, Fig. 3]. We assume that all the users are in the reflection space of the RIS to show the impact of RIS and RS on the EE of the users. As can be observed, RIS can significantly improve the EE of the system. Moreover, it can be observed that IQI can highly degrade the system performance if it is not considered in the system design. Note that the IQI-unaware scheme employs proper Gaussian signaling with random RIS components, while the other schemes employ IGS. We also observe that RS can considerably outperform TIN from an EE point of view.

Fig. 3 shows the average fairness EE versus P_c for $N_{BS} = N_u = 2$, $L = 1$, $M = 1$, $K = 8$ and $N_{RIS} = 100$. In this figure, we compare the performance of a regular RIS with a STAR-RIS in a single-cell BC. To this end, we assume that both regular and STAR-RISs employ the same number of RIS components. We also assume that half of the users are in the reflection space and the other half are in the transmission space
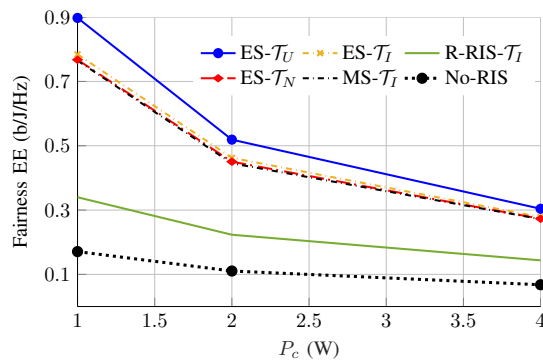
Fig. 3: The average fairness EE versus P_c for $N_{BS} = N_u = 2$, $L = 1$, $M = 1$, $K = 8$ and $N_{RIS} = 100$.

of RISs, meaning that the regular RIS can cover only half of users, while the STAR-RIS can assist all the users. As can be observed, RIS can highly enhance EE even when the regular RIS is unable to cover all the users, Furthermore, STAR-RIS can significantly outperform a regular RIS. The benefits of STAR-RIS increase with the number of users and the number of RIS components. Additionally, we observe that STAR-RIS with the MS scheme with a unit modulus constraint performs close to the ES scheme with $\mathcal{T}_I$ and $\mathcal{T}_N$.

V. CONCLUSION

We proposed energy-efficient schemes for multi-cell STAR-RIS BCs by employing RS and IGS. We considered imperfect devices, suffering from IQI. We showed that RIS can significantly improve the EE of the system. Additionally, we showed that STAR-RIS can highly outperform a regular RIS when the regular RIS is unable to cover all the users. Moreover, we showed that RS can enhance the EE of the system. Finally, our results show that IQI can highly degrade the EE of the system when it is not compensated in the design.

ACKNOWLEDGMENT

REFERENCES

[1] T. Gong *et al.*, "Holographic MIMO communications: Theoretical foundations, enabling technologies, and future directions," *arXiv preprint arXiv:2212.01257*, 2022.

[2] Q. Wu *et al.*, "Intelligent reflecting surface aided wireless communications: A tutorial," *IEEE Trans. Commun.*, vol. 69, no. 5, pp. 3313–3351, 2021.

[3] M. Di Renzo *et al.*, "Smart radio environments empowered by reconfigurable intelligent surfaces: How it works, state of research, and the road ahead," *IEEE J. Sel. Areas Commun.*, vol. 38, no. 11, pp. 2450–2525, 2020.

[4] Y. Mao *et al.*, "Rate-splitting multiple access: Fundamentals, survey, and future research trends," *IEEE Commun. Surv. Tutor.*, vol. 24, no. 4, pp. 2073–2126, 2022.

[5] C. Huang *et al.*, "Reconfigurable intelligent surfaces for energy efficiency in wireless communication," *IEEE Trans. Wireless Commun.*, vol. 18, no. 8, pp. 4157–4170, 2019.

[6] Q. Wu and R. Zhang, "Intelligent reflecting surface enhanced wireless network via joint active and passive beamforming," *IEEE Trans. Wireless Commun.*, vol. 18, no. 11, pp. 5394–5409, 2019.

[7] C. Pan *et al.*, "Multicell MIMO communications relying on intelligent reflecting surfaces," *IEEE Trans. Wireless Commun.*, vol. 19, no. 8, pp. 5218–5233, 2020.

[8] M. Soleymani, I. Santamaria, and P. J. Schreier, "Improper signaling for multicell MIMO RIS-assisted broadcast channels with I/Q imbalance," *IEEE Trans. Green Commun. Netw.*, vol. 6, no. 2, pp. 723–738, 2022.

[9] K. Weinberger *et al.*, "Synergistic benefits in IRS-and RS-enabled C-RAN with energy-efficient clustering," *IEEE Trans. Wireless Commun.*, vol. 21, no. 10, pp. 8459–8475, 2022.

[10] T. Jiang and W. Yu, "Interference nulling using reconfigurable intelligent surface," *IEEE J. Sel. Areas Commun.*, 2022.

[11] I. Santamaria *et al.*, "Interference leakage minimization in RIS-assisted MIMO interference channels," in *Proc. IEEE Int. Conf. on Acoust., Speech and Signal Process. (ICASSP)*, 2023.

[12] J. Xu, Y. Liu, X. Mu, R. Schober, and H. V. Poor, "STAR-RISs: A correlated T&R phase-shift model and practical phase-shift configuration strategies," *IEEE J. Sel. Topics Signal Process.*, pp. 1–1, 2022.

[13] Y. Liu, X. Mu, R. Schober, and H. V. Poor, "Simultaneously transmitting and reflecting (STAR)-RISs: A coupled phase-shift model," in *Proc. IEEE Int. Conf. Commun. (ICC)*. IEEE, 2022, pp. 2840–2845.

[14] X. Mu, Y. Liu, L. Guo, J. Lin, and R. Schober, "Simultaneously transmitting and reflecting (STAR) RIS aided wireless communications," *IEEE Trans. Wireless Commun.*, vol. 21, no. 5, pp. 3083–3098, 2022.

[15] J. Xu *et al.*, "STAR-RISs: Simultaneous transmitting and reflecting reconfigurable intelligent surfaces," *IEEE Commun. Lett.*, vol. 25, no. 9, pp. 3134–3138, 2021.

[16] M. Soleymani, I. Santamaria, and E. Jorswieck, "Spectral and energy efficiency maximization of MISO STAR-RIS-assisted URLLC systems," *arXiv preprint arXiv:2301.00583*, 2023.

[17] ——, "Rate splitting in MIMO RIS-assisted systems with hardware impairments and improper signaling," *IEEE Trans. Veh. Technol.*, vol. 72, no. 4, pp. 4580–4597, April 2023.

[18] M. Soleymani, I. Santamaria, E. Jorswieck, and S. Rezvani, "NOMA-based improper signaling for multicell MISO RIS-assisted broadcast channels," *IEEE Trans. Signal Process.*, vol. 71, pp. 963–978, 2023.

[19] M. Soleymani, I. Santamaria, B. Maham, and P. J. Schreier, "Rate region of the K-user MIMO interference channel with imperfect transmitters," in *Proc. IEEE Eu. Signal Process. Conf. (EUSIPCO)*, 2020, pp. 1–5.

[20] M. Soleymani *et al.*, "Improper Gaussian signaling for the K-user MIMO interference channels with hardware impairments," *IEEE Trans. Veh. Technol.*, vol. 69, no. 10, pp. 11 632–11 645, 2020.

[21] S. Javed, O. Amin, S. S. Ikki, and M.-S. Alouini, "Multiple antenna systems with hardware impairments: New performance limits," *IEEE Trans. Veh. Technol.*, vol. 68, no. 2, pp. 1593–1606, 2019.

[22] V. R. Cadambe *et al.*, "Interference alignment with asymmetric complex signaling–Settling the Høst-Madsen-Nosratinia conjecture," *IEEE Trans. Inf. Theory*, vol. 56, no. 9, pp. 4552–4565, 2010.

[23] M. Soleyman *et al.*, "Energy-efficient design for underlay cognitive radio using improper signaling," in *Proc. IEEE Int. Conf. on Acoust., Speech and Signal Processing (ICASSP)*, 2019, pp. 4769–4773.

[24] M. Soleymani *et al.*, "Improper signaling for SISO two-user interference channels with additive asymmetric hardware distortion," *IEEE Trans. Commun.*, vol. 67, no. 12, pp. 8624–8638, 2019.

[25] M. Soleymani, I. Santamaria, and E. Jorswieck, "Rate region of MIMO RIS-assisted broadcast channels with rate splitting and improper signaling," in *Proc. IEEE 26th Int. ITG Workshop Smart Antennas & 13th Conf. Syst., Commun., and Coding (WSA & SCC)*, 2023, pp. 1–6.

[26] S. Javed, O. Amin, B. Shihada, and M.-S. Alouini, "A journey from improper Gaussian signaling to asymmetric signaling," *IEEE Commun. Surv. Tutor.*, vol. 22, no. 3, pp. 1539–1591, 2020.

[27] Y. Liu *et al.*, "STAR: Simultaneous transmission and reflection for 360 coverage by intelligent surfaces," *IEEE Wireless Commun.*, vol. 28, no. 6, pp. 102–109, 2021.

[28] A. Zappone and E. Jorswieck, "Energy efficiency in wireless networks via fractional programming theory," *Found Trends® in Commun. Inf. Theory*, vol. 11, no. 3-4, pp. 185–396, 2015.